INVITED PAPER

Tail Control Enhances Gliding in Arboreal Lizards: An Integrative Study Using a 3D Geometric Model and Numerical Simulation

Complimentary/Contributed Paper

Jaden Clark,[1,*] Christopher Clark[†] and Timothy E. Higham [ID][‡]

*Department of Engineering, Stanford University, Stanford, CA 94305, USA; [†]Department of Engineering, Harvey Mudd College, Claremont, CA 91711, USA; [‡]Department of Evolution, Ecology, and Organismal Biology, University of California, Riverside, CA 92521, USA

[1]E-mail: jvclark@stanford.edu

Synopsis The ability to glide through an arboreal habitat has been acquired by several mammals, amphibians, snakes, lizards, and even invertebrates. Lizards of the genus *Draco* possess specialized morphological structures for gliding, including a patagium, throat lappets, and modified hindlimbs. Despite being among the most specialized reptilian gliders, it is currently unknown how *Draco* is able to maneuver effectively during flight. Here, we present a new computational method for characterizing the role of tail control on *Draco* glide distance and stability. We first modeled *Draco* flight dynamics as a function of gravitational, lift, and drag forces. Lift and drag estimates were derived from wind tunnel experiments of 3D printed models based on photos of *Draco* during gliding. Initial modeling leveraged the known mass and planar surface area of the *Draco* to estimate lift and drag coefficients. We developed a simplified, 3D simulation for *Draco* gliding, calculating longitudinal and lateral position and a pitch angle of the lizard with respect to a cartesian coordinate frame. We used PID control to model the lizards' tail adjustment to maintain an angle of attack. Our model suggests an active tail improves both glide distance and stability in *Draco*. These results provide insight toward the biomechanics of *Draco*; however, future *in vivo* studies are needed to provide a complete picture for gliding mechanics of this genus. Our approach enables the replication and modification of existing gliders to better understand their performance and mechanics. This can be applied to extinct species, but also as a way of exploring the biomimetic potential of different morphological features.

Introduction

Arboreal habitats are inundated with a complex 3D array of branches and surfaces. In addition to the structural variation in the physical parts of the trees, there are also gaps of variable sizes. Although some animals can simply avoid these gaps and move exclusively on trees, many animals will execute maneuvers to cross these gaps. In these cases, being able to bridge these gaps while avoiding injury is crucial for survival in these habitats. Whereas some animals simply fall from an arboreal surface in a controlled way (e.g., Yanoviak et al. 2005; Higham et al. 2017), many vertebrates have evolved specialized morphology and behavior to cross the gaps. These strategies can include reaching, swinging, leaping, and gliding (Günther et al. 1991; Demes et al. 1995; Hunt et al. 1996; Byrnes and Jayne 2012; Graham and Socha 2020). Of these strategies, gliding is likely the most effective for crossing large gaps.

To glide effectively from one place to another, animals often exhibit morphological, physiological, and behavioral specializations. Squirrel and lizard gliders use patagia, and frogs use enlarged feet and webbings to increase lift (Gupta 1966; Emerson and Koehl 1990; Russell et al. 2001). Snakes undulate in mid-air to dynamically adjust their aerodynamics (Socha 2002; Socha et al. 2005; Yeaton et al. 2020). These biomechanical phenomena can be challenging to study, but they provide important insight into the evolution of gliders, as well as the development of

biomimetic robots (Yanoviak et al. 2005; Shin et al. 2018).

Among reptiles, several groups have modified morphological features that assist with directed descents (Dudley et al. 2007). For example, geckos from Southeast Asia, including *Ptychozoon*, *Luperosaurus*, and *Cosymbotus*, have fully webbed hands and feet, along with dorsoventrally flattened tails and flaps (or folds) of skin along the lateral edges of the body (Russell 1979; Brown et al. 2000; Russell and Dijkstra 2001). Lizards of the agamid genus *Draco* are some of the most advanced reptilian gliders (Herre 1958; Mcguire and Dudley 2011). A modified patagium, as well as throat lappets and modified hindlimbs help *Draco* maximize their aerodynamic lift during gliding (Colbert 1967; Russell and Dijkstra 2001; Mcguire 2003). Their musculoskeletal anatomy, including elongate ribs and modified muscles, is also specialized to modulate the position of the patagium (Colbert 1967).

Like many other Southeast Asian and Indian vertebrates, *Draco* likely developed their specialized gliding morphology as a result of dipterocarp forest development, which is characterized by large trees and tall, open canopies (Heinicke et al. 2012). Now, *Draco* is composed of over 45 species, which range significantly in both size and gliding performance (Mcguire and Heang 2001). It is thought that the ability to control trajectory during aerial descent is a major driver in the evolution of gliding flight (Smith 1952; Yanoviak et al. 2005). Despite research on comparative glide distance and motion planning in *Draco*, the mechanism through which *Draco* controls its aerial trajectory is largely unknown (Mcguire 2003; Mcguire and Dudley 2005; Khandelwal and Hedrick 2020).

Recent research has shown that the tail can play a significant role in lizard locomotory stability and reorientation (Gillis et al. 2009; Libby et al. 2012; Gillis and Higham 2016). Specifically, geckos are able to self-right during free-fall and adjust their yaw during gliding with the tail alone (Jusufi et al. 2008, 2010). In addition, other lizards within the family Agamidae use the tail to ensure pitch stability during jumping (Libby et al. 2012). Similarly, flying squirrels of the genus *Glaucomys* are thought to use the tail to stabilize their pitch (Dudley et al. 2007; Hayssen 2008). However, tail function during gliding in *Draco*, arguably the most proficient gliding reptile, has not been examined. Prior studies on *Draco* have relied on observations of glide behavior in videos, and they show significant pitch and yaw movement of the tail during landing and maneuvering in gliding (Fig. 1).

The goals of this study are to determine (1) the aerodynamic properties of *Draco*'s gliding morphology and (2) the role of the tail in pitch stability and glide performance. A three degree-of-freedom model of *Draco* gliding dynamics is presented. We organize our methods into three distinct processes: (1) construction of a glide dynamics model, (2) construction of a 3D geometric model and parameter estimation, and (3) numerical simulation. This methodology was successful in determining aerodynamic parameters of a 3D geometric *Draco* model, and characterizing the effect of tail control on *Draco* flight stability and glide distance. We hypothesized that an active tail will improve *Draco* glide stability and distance.

Materials and methods

Museum specimens

We quantified the relative size of the tail and body of two species of *Draco* from the collection of Lee Grismer at La Sierra University. A digital scale was used to measure mass and photographs (dorsal view with limbs in the plane of the body) were taken of each specimen for additional measurements. ImageJ was used to quantify lengths and centroid. The latter was quantified by first outlining the lizard using the freehand tool. The centroid was then the average of the x and y coordinates of all of the pixels in the selection. Finally, the center of mass was determined by balancing the stiff (preserved) lizard on a thin rod. The fore-aft location that resulted in a balanced lizard was noted and then measured. Total body (with tail) masses of *D. fimbriatus*, and *D. maculatus* were 18.5 and 5.9 g, respectively. The tail for the two species represented 6.5% and 8.5% of total body mass, respectively.

The snout–vent length (SVL) and tail length of *D. fimbriatus* was 10.50 and 18.38 cm, respectively. The centroid (without tail) was 6.95 cm from the tip of the snout (66% of SVL). The SVL and tail length of *D. maculatus* was 7.69 and 12.02 cm, respectively. The centroid (without tail) was 5.02 cm from the tip of the snout (65% of SVL). In contrast, the center of mass was approximately 54% of SVL (from the tip of the snout) in all species.

Mathematical model of motion

A pitching dynamics model was developed to characterize the effects of lift, drag, and weight forces on the lizard's motion. The aerodynamic model was similar to that of Yeaton et al. (2017), however, the lift and drag coefficients were experimentally determined as opposed to extracted from a characteristic

Fig. 1. *Draco* shows significant tail movement during gliding (Image from J. M. Dehling on creative commons).

model. The lizard is modeled as two rigid rods, connected via a rotational joint located at the end of each rod. The tail was designed to pivot about the ventral end of the lizard's torso, adjusting its center of mass and inertia. In Jusufi et al. (2010), aerial reorientation of geckos is modeled using the conservation of momentum. In this work, the model is generated using Newtonian dynamics of the system, that is, the net forces and torques (e.g., from lift, and drag) on the lizard are balanced to compute acceleration, velocity, and position/orientation states.

Using the free-body diagram in Fig. 2, we defined horizontal, vertical, and rotational equations of motion:

$$m_{\text{tot}}\ddot{x} = -L\sin(\theta - \alpha) - D\cos(\theta - \alpha). \quad (1)$$

$$m_{\text{tot}}\ddot{y} = -Mg - mg - D\sin(\theta - \alpha) + L\cos(\theta - \alpha). \quad (2)$$

$$I\ddot{\theta} = -r_1 D\sin(\alpha) - r_1 L\cos(\alpha) + r_2 mg\cos(\theta) + I_{\text{tail}}\alpha_{\text{tail}}. \quad (3)$$

where m_{tot} is the total mass, g is the gravitational acceleration, M and m are the body and tail masses, L and D are the lift and drag forces, and θ and α are the angles of attack and pitch. r_1 and r_2 were defined as the distance from the body's center-of-mass to the center of pressure, and the distance from the tail's center-of-mass to the center-of-pressure. I_{tail} was the inertia of the tail, and α_{tail} was the angular acceleration of the tail. We assumed the moment of inertia of both the lizard's body and tail as costs and modeled them as solid rods. By definition, lift is the aerodynamic force normal to the direction of

motion, and drag is that parallel to the direction of the motion in still air. Pitch is the angle of the lizard relative to the horizontal plane, and the angle of attack is the angle of the lizard relative to its direction of motion.

3D geometric model

To determine the lift and drag of *Draco*, a 3D geometric model was developed in Blender based on photographs of *Draco dussumieri* mid-flight (Dehling 2017). The 3D geometric model was designed to reflect the geometry of *Draco* during the equilibrium phase of the glide, as opposed to the landing or takeoff phases (Fig. 3). Photographs from the gliding phase were prioritized as *Draco* employs landing and takeoff specific mechanisms during their respective phases as seen in Fig. 4 (Khandelwal and Hedrick 2020).

Wind tunnel experimentation

To determine aerodynamic characteristics, experiments were run on the 3D geometric *Draco* model in a custom-built Harvey Mudd College wind tunnel designed for teaching and research. This wind tunnel was a closed circuit and has a rectangular cross-section with a height and width of 31 cm. The working distance was 60 cm and the wind tunnel was completely horizontal with respect to the ground. The 3D geometric model was affixed to an linear variable differential transformer (LVDT) transducer facing into the direction of fluid flow. The 3D geometric model was rotated to provide different angles of attack. The LVDT measured forces normal and parallel to the wind's direction, which correlated with lift and drag measurements, respectively. Airspeed was measured with a pitot tube using a Dwyer Series 475 Mark III Digital Manometer, and the angle of attack was measured using basic trigonometry based on the configuration described in Fig. 5.

Lift and drag were measured at airspeeds ranging from 3 to 34 m/s at angles of attack between $-15°$ and $35°$. These airspeeds produced Reynolds numbers in the range of 13,000–220,000. Reynolds numbers tested at higher speeds significantly exceeded values reported for both *Draco maculatus* (Re ∼ 20,300) and *Draco fimbriatus* (Re ∼ 36,000). Although these speeds are unrealistic for *Draco* to attain, Reynolds numbers between 10^3 and $4*10^5$ (for bluff bodies, and higher for streamlined bodies) generally produce similar aerodynamic coefficients (Hoerner 1965; Vogel 1994). Lift and drag coefficients were calculated as a function of angle of attack based on the following equations:
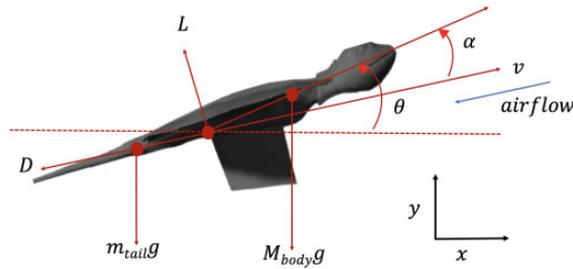
Fig. 2. The free-body-diagram describing the pitching dynamics of *Draco*. Here, $M_{body}g$ and $m_{tail}g$ are the weight forces from the body and tail, L and D are the lift and drag forces, and θ and α are the angle-of-attack and pitch. v represents the velocity of lizard, which is antiparallel to the direction of airflow relative to the lizard.

$$C_D = \frac{2D}{\rho v^2 A}. \qquad (4)$$

$$C_L = \frac{2L}{\rho v^2 A}. \qquad (5)$$

in which D and L are the drag and lift, C_D and C_L are the drag and lift coefficients, ρ is the density, v is the velocity of the air, and A is the reference area of the lizard. The reference area was defined as the frontal portion of the 3D geometric model directly exposed to the oncoming fluid.

Numerical simulation and tail control

We sought to understand the role of tail activity on *Draco* glide stability. To do this a reduced-order gliding simulation was developed in Matlab based on our pitching dynamics model (Fig. 2) and experimentally determined lift and drag coefficients. Glide paths were simulated from a starting height of 5 m, and glide distance was computed based on the

horizontal distance a lizard had traveled upon reaching a height of 0 m. The lizard was initially horizontal (a pitch angle of 0) with no angular velocity, and with a horizontal velocity of 2.5 m/s. Each timestep was 0.001 s.

This technique has previously been used to evaluate non-equilibrium gliding in vertebrate gliders and characterize gliding squirrel flight (Yeaton et al. 2017; Zhao et al. 2019). Reduced order simulations have also proven useful to understand the use of tail as an inertial appendage for self-righting (Jusufi et al. 2010). However, this approach has not been utilized to study *Draco* flight. Moreover, the work presented here extends such work to include a feedback control system that tracks tail angle as a function of a desired angle of attack.

The relative location of the center-of-pressure of an aerofoil is an important factor in flight stability. In typical aerofoils with limited control structures, when the centroid is aft to the center-of-mass, an aerofoil is often aerodynamically unstable (Anderson 2001). Aerofoils with a more fore centroid are often easier to control due to self-stabilizing aerodynamic forces. Based on measurements from museum specimens, the center-of-pressure likely lies very close to (within ∼0.01 m of) the center-of-mass. This means that behavior likely plays a role in flight stability, as small changes in *Draco* posture during gliding could change the relative locations of the center-of-pressure, and center-of-mass. Tail activity is one way *Draco* could shift its center-of-mass during gliding.

In the simulation, the tail was set to adjust the angle between −90° and 90° with respect to the lizard's body length about a pivot on the ventral end of the lizard (Fig. 6). This resulted in corresponding changes in the location of the tail's center of mass. Tail angle was modulated using a
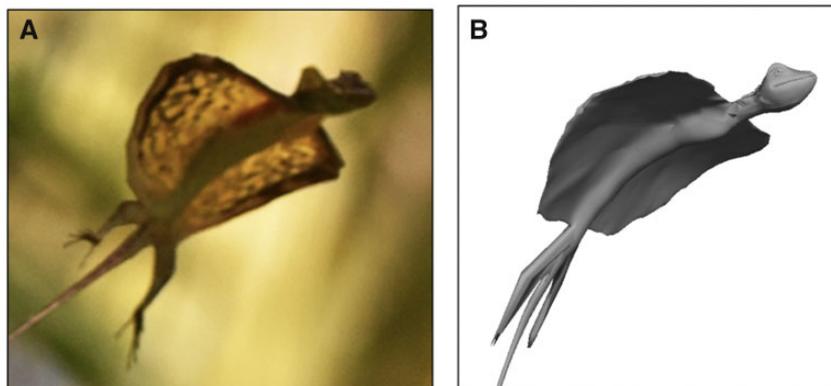
Fig. 3. The *Draco* 3D geometric model (**A**) was developed in Blender based on *Draco* gliding morphology (**B**). (Image from J. M. Dehling on creative commons).
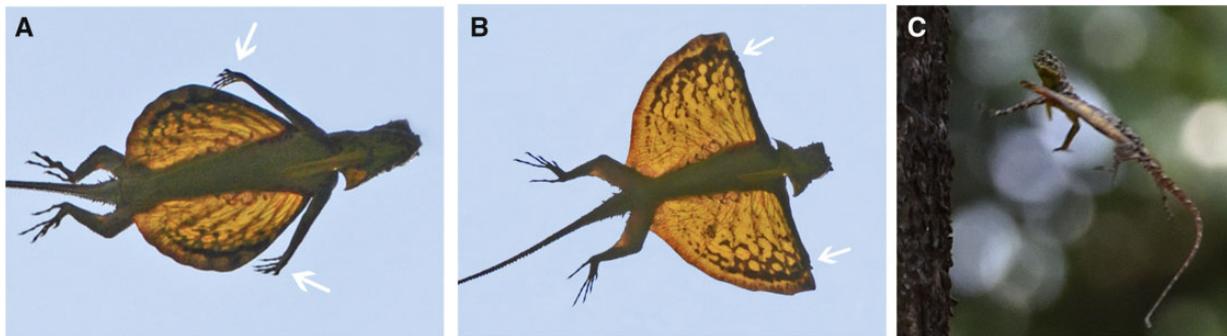
Fig. 4. A 3D geometric model was developed based on photos of the equilibrium phase of *Draco* gliding (**B**). *Draco* also adjusts its gliding morphology during the takeoff phase (**A**) and the landing phase (**C**). (Images from J. M. Dehling on creative commons).
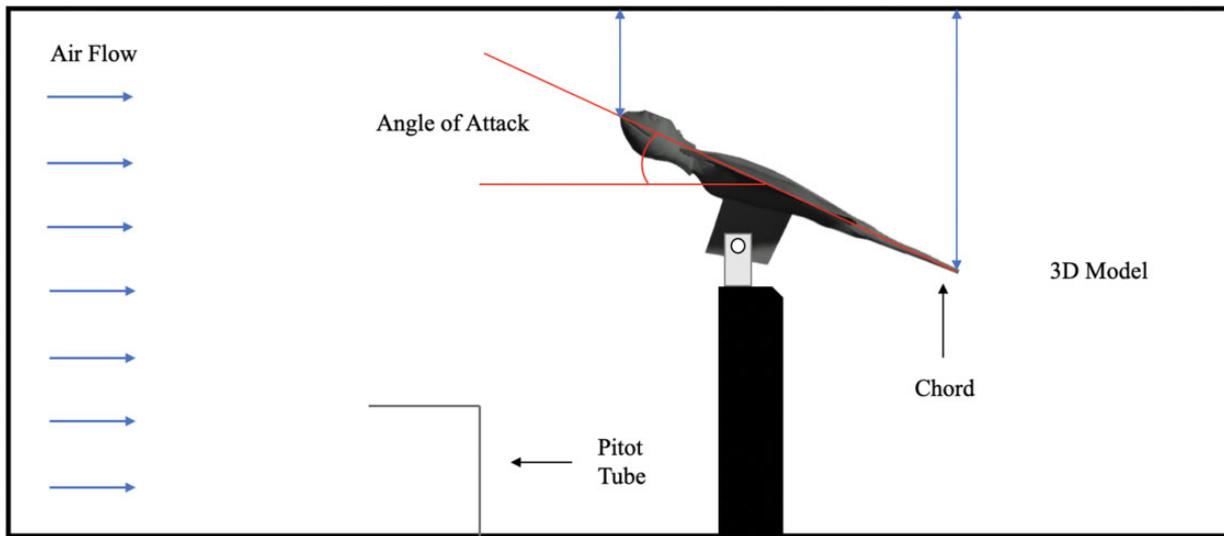
Fig. 5. Wind tunnel experiments were performed to determine lift and drag coefficients of *Draco*. The 3D geometric model was affixed to an LVDT transducer facing into the direction of fluid flow. The 3D geometric model was rotated to provide different angles of attack. The LVDT measured forces normal and parallel to the wind's direction, which correlated with lift and drag measurements, respectively. Airspeed was measured with a pitot tube using a Dwyer Series 475 Mark III Digital Manometer.

proportional–integral–derivative (PID) controller designed to track the angle of attack. PID controllers are standard in many control systems. The controller accepts the desired output (in this case an angle of attack) and modulates an input to minimize the difference between the actual and desired output based on PID responses:

$$e = \alpha_{\text{desired}} - \alpha. \quad (6)$$

$$\theta_{\text{tail}} = \theta_{\text{tail}} + k_p e + k_d \dot{e} + k_i \int e \, dt \quad (7)$$

in which k_p, k_d, and k_i are the control coefficients, α is the angle of attack, and e is the error. θ_{tail} was the tail angle. An error was defined as the difference between the desired angle of attack and the actual angle of attack at the previous timestep. Maximum angular velocity of

the tail was approximated based on data from aerial reorientation in geckos (Jusufi et al. 2010).

To characterize the role of tail activity on glide performance, simulations on models with an active tail (using the PID controller), a rigid tail, and no tail were performed. In addition, the effect of different relative tail and mass lengths on glide distance was examined. To better understand the aerodynamics of *Draco* morphology, simulations were also performed to determine the effect of angle of attack on glide distance.

Results

Lift and drag coefficients

The wind tunnel experiments (see the "Wind tunnel experimentation" section) produced the following lift and drag curves (Fig. 7):
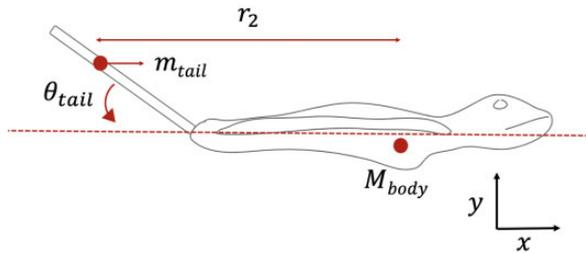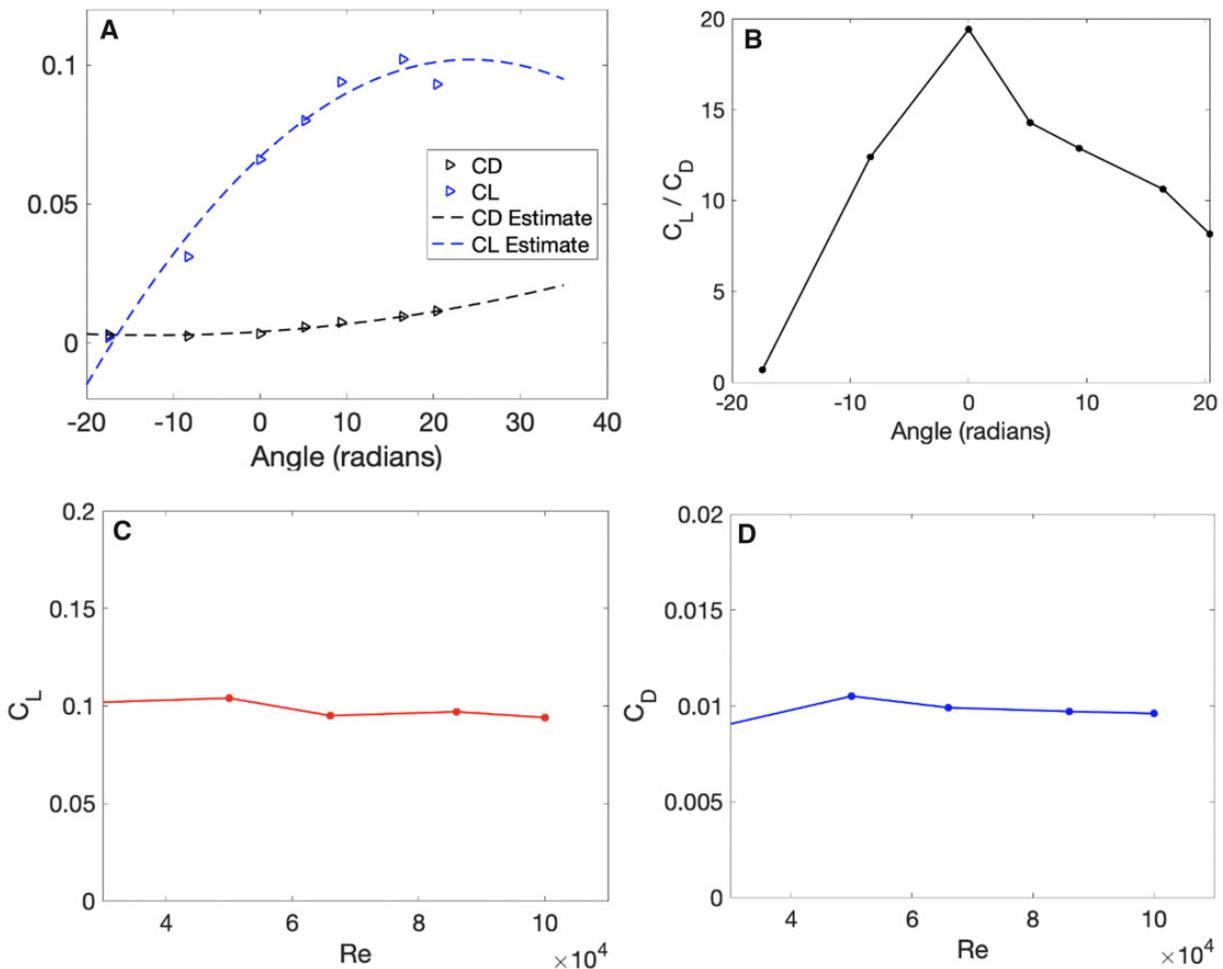
Fig. 6. Tail angle (θtail) was controlled to track a desired angle-of-attack. The distance ($r2$) of the tail center-of-mass ($m$tail) changes relative to body center-of-mass (Mbody) when the tail angle changes.

$$C_D = 0.000008\alpha^2 + 0.0002\alpha + 0.004 \quad R^2 = 0.9868 \quad (8)$$
$$C_L = -0.00006\alpha^2 + 0.0029\alpha + 0.0669 \quad R^2 = 0.9789 \quad (9)$$

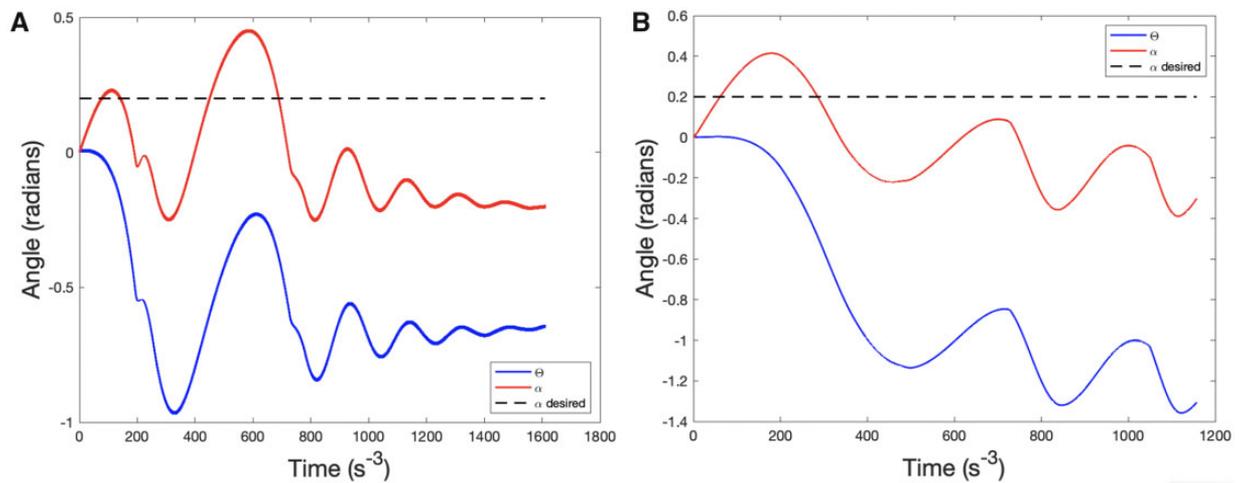in which α represents the 3D geometric model's angle of attack.

Effectiveness of tail controller

PID control coefficients were determined based on an exhaustive search to minimize the mean-squared error of angle of attack in the last 2 s of a glide.

Draco maculatus had a mean-squared error in angle of attack of 0.163 square radians. *Draco fimbriatus* had a mean-squared error in angle of attack of 0.271 square radians over the last 2 s of its glide (Fig. 8).

Active versus rigid versus no tail

Both *D. maculatus* and *D. fimbriatus* glided farthest with the active tail, than the rigid tail, and finally with no tail. *Draco maculatus* glided 8.29 m with active tail control, 3.64 m with a rigid tail, and 2.43 m with no tail (Fig. 9). *Draco fimbriatus* glided 4.16 m with active tail control, 2.93 m with a rigid tail, and 2.40 m with no tail (Figs. 10 and 11).

Fig. 7. Lift and drag coefficients were measured in a wind tunnel at speeds ranging from 3 to 30 m/s as a function of angle of attack. The drag and the lift coefficients were estimated as a quadratics function relative to angle of attack (**A**). Panel **B** depicts the lift coefficient (C_L) to drag coefficient (C_D) ratio as a function of angle of attack. Effect of Reynolds number (Re) on lift coefficient (**C**) and drag coefficient (**D**) at an angle of attack of $16.4°$ are also depicted.

Fig. 8. *Draco maculatus* (**A**) and *D. fimbriatus* (**B**) angle-of-attack control was simulated using an active tail. Angle of attack (α) is depicted in red, and lizard pitch (θ) is depicted in blue. The tail angle was adjusted to track a desired angle of attack. *Draco maculatus* had a mean-squared error in the angle of attack of 0.163. *Draco fimbriatus* had a mean-squared error in the angle of attack of 0.271 square radians over the last 2 s of its glide.
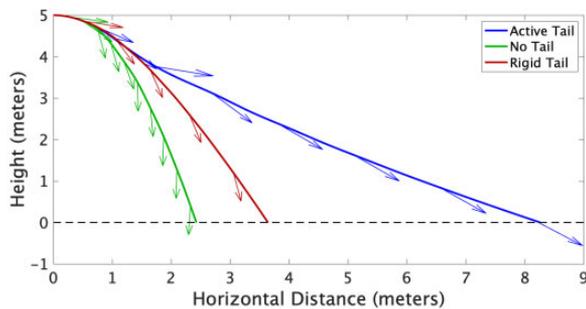
Fig. 9. To characterize the role of tail activity on glide performance in *Draco*, simulations on models with an active tail (using the PID controller), a rigid tail, and no tail were performed. From a height of 5 m, *D. maculatus* glided 8.29 m with active tail control, 3.64 m with a rigid tail, and 2.43 m with no tail.

Fig. 10. To characterize the role of tail activity on glide performance in *Draco*, simulations on models with an active tail (using the PID controller), a rigid tail, and no tail were performed. From a height of 5 m, *D. fimbriatus* glided 4.16 m with active tail control, 2.93 m with a rigid tail, and 2.40 m with no tail.

Discussion

Gliding is the use of control features to direct an animal horizontally during aerial descent (Socha et al. 2015). Among lizards, some geckos and agamids have the ability to glide, and this is facilitated by morphological specializations of the body, feet, and tail (Young et al. 2002). Our integrative study examined gliding performance in two species of *Draco* that vary in gliding ability. We found that glide distances in our simulation parallel those found by Mcguire and Dudley (2005) when they studied gliding performance in a number of *Draco* species. In that study, *Draco* was coaxed to fly between poles 9.3 m apart from a 6 m tall pole, which was referred to as a "comfortable" gliding distance. Lizards lost between 2.6 and 6.2 m over the course of the 9.3-m glide.
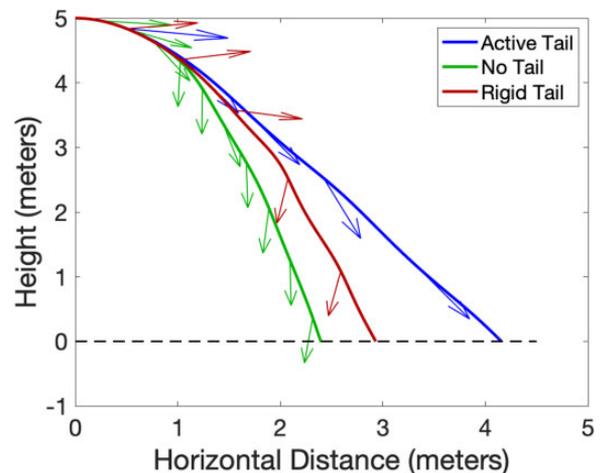
Our simulation produced a glide distance of 4.16 m for *D. fimbriatus* and 8.29 m for *D. maculatus* from a starting height of 5 m. These distances fall slightly short of the maximum glide distances in the same species during live tests, however, these simulations only accounted for the tail as a control structure. Adjustment of the camber of the patagium and other control strategies could further improve actual glide distance in *Draco*. As a result, we conclude that the tail is effective in improving glide distance in *Draco*, but other control strategies may also be used to enhance performance.
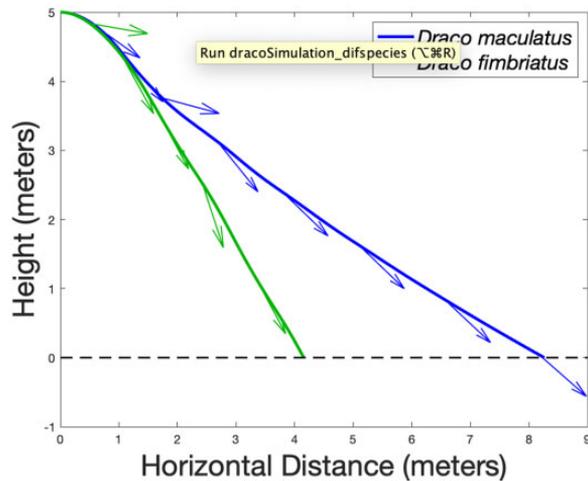
Fig. 11. We compared glide distance of *D. fimbriatus* and *D. maculatus* during glide simulations with an active tail. From a height of 5 m, *D. fimbriatus* glided 4.16 and *D. maculatus* glided 8.29 m.

Given the similarity between the previous empirical measurements and our simulations, our approach could be used to predict maximum glide distance. This has great utility for studies that are limited by enclosure size during laboratory experiments, and for studies involving species for which empirical data are difficult to obtain. These simulations might also serve as a measure of maximum performance, which can then be compared with the actual performance employed during gliding in nature. This is especially important given that lizards often underperform under natural conditions (e.g., Irschick and Losos 1998).

Role of the tail

Tails are critical for numerous ecologically-relevant behaviors such as prey capture, climbing, running, jumping, maneuvering, and maintaining stability (Gillis et al. 2009; Jusufi et al. 2010; Gillis and Higham 2016; M. F. Vollin and T. E. Higham, submitted for publication). The tail function is often studied by capitalizing on the innate ability of most lizards to self-amputate their tail (autotomy). However, this is not always possible since not all lizards are capable of autotomy. Our geometric model, wind tunnel experiments, and numerical simulation revealed how active tails can enhance gliding performance. This approach may be used as a surrogate for tail autotomy studies, especially for those species lacking that ability. Given that the role of tails during aerial locomotion is poorly understood, especially for gliding reptiles, our study is a potential aid for understanding tail function.

Tails are used to enhance aerial behavior in several vertebrates. Examples include gliding in squirrels and righting and mid-air turning in geckos (Jusufi et al. 2010), among others. The ability to control aerial descent is thought to be associated with the evolution of gliding and flapping flight (Yanoviak et al. 2005). Our simulation demonstrated that *D. maculatus* can significantly improve glide distance using tail control. However, while tail control slightly improved the gliding distance of *D. fimbriatus*, it did not effectively stabilize the angle of attack in this simulation. Based on past work, *D. fimbriatus* is a relatively poor glider due to its high mass and consequent wing-loading (Mcguire 2003). As a result, it makes sense to conclude that this species may also struggle to maneuver and stabilize during gliding.

Limitations

It should be noted that the 3D geometric model does not accurately represent certain aspects of *Draco* morphology. The 3D geometric printed model is rigid and smooth. However, *Draco* has rough scales which may influence boundary layer aerodynamics on the patagium (Vogel 1994). In addition, *Draco* has been hypothesized to adjust their camber during flight (Mcguire and Dudley 2005; Dehling 2017), whereas the 3D geometric model has a fixed camber.

Our simulation is limited in that it only takes into account the tail as a control structure for gliding. Other studies have suggested that there is significant camber adjustment during gliding (Mcguire and Dudley 2005; Dehling 2017). *Draco* also likely uses their forelimbs to manipulate the patagium, which could influence aerial maneuverability (Dehling 2017). *Draco* also possesses modified hindlimbs to increase lift, which could be used for flight control. Future *in vivo* studies are needed to mechanistically study the roles of these control structures during *Draco* gliding.

In addition, this work did not consider the aerodynamics associated with tail movement. Also, the tail and body were modeled as solid rods. Future simulations should more accurately measure the inertia of *Draco* body and tail.

Conclusion

In this study, we used computational methods to quantify gliding flight control in *Draco* using a custom-developed 3D geometric model, wind tunnel experiments, and numerical simulation. We determined that tail control can be used to improve glide distance and stability in both *D. maculatus* and *D. fimbriatus*. We also corroborated past results

showing that species with higher wing-loading (*D. fimbriatus*) have shorter maximum glide distances (Mcguire 2003).

In the future, we believe this methodology could be useful for studying the control of gliding flight, the role of autotomy on locomotion in lizards, and the evolution of gliding in reptiles. In regards to the latter, it is unclear how much control early gliders had over their tail, but we assume that both gliding ability and tail control likely evolved in parallel. Applying our approach to reconstructed extinct specimens would provide insight into the gliding ability of these species.

Conflicts of interest

The authors declare no conflicts of interest.

Data availability

Data and simulation code for this article is available at https://github.com/jadenvc/Active-tails-enhance-gliding-in-arboreal-lizards-.

References

Anderson JD. 2001. Fundamentals of aerodynamics. Boston (MA): McGraw-Hill.

Brown RM, Supriatna J, Ota H. 2000. Discovery of a new species of Luperosaurus (Squamata; Gekkonidae) from Sulawesi, with a phylogenetic analysis of the genus, and comments on the status of *Luperosaurus serraticaudus*. Copeia 2000:191–209.

Byrnes G, Jayne BC. 2012. The effects of three-dimensional gap orientation on bridging performance and behavior of brown tree snakes (*Boiga irregularis*). J Exp Biol 215:2611–20.

Colbert EH. 1967. Adaptations for gliding in the lizard *Draco*. Am Mus Novit 2283:1–20.

Dehling JM. 2017. How lizards fly: a novel type of wing in animals. PLoS ONE 12:e0189573.

Demes B, Jungers WL, Gross TS, Fleagle JG. 1995. Kinetics of leaping primates: influence of substrate orientation and compliance. Am J Phys Anthropol 96:419–29.

Dudley R, Byrnes G, Yanoviak SP, Borrell B, Brown RM, Mcguire JA. 2007. Gliding and the functional origins of flight: biomechanical novelty or necessity? Annu Rev Ecol Evol Syst 38:179–201.

Emerson SB, Koehl MA. 1990. The interaction of behavioral and morphological change in the evolution of a novel locomotor type "Flying" frogs. Evolution 44:1931.

Gillis GB, Bonvini LA, Irschick DJ. 2009. Losing stability: tail loss and jumping in the arboreal lizard *Anolis carolinensis*. J Exp Biol 212:604–9.

Gillis G, Higham TE. 2016. Consequences of lost endings: caudal autotomy as a lens for focusing attention on tail function during locomotion. J Exp Biol 219:2416–22.

Graham M, Socha JJ. 2020. Going the distance: the biomechanics of gap-crossing behaviors. J Exp Zool Part A Ecol Integr Physiol 333:60–73.

Günther MM, Ishida H, Kumakura H, Nakano Y. 1991. The jump as a fast mode of locomotion in arboreal and terrestrial biotopes. Z Morphol Anthropol 78:341–72.

Gupta BB. 1966. Notes on the gliding mechanism in the flying squirrel. Occasional papers of the. museum. Zool Univ Mich 645:1–7.

Hayssen V. 2008. Patterns of body and tail length and body mass in sciuridae. J Mammal 89:852–73.

Heinicke MP, Greenbaum E, Jackman TR, Bauer AM. 2012. Evolution of gliding in Southeast Asian geckos and other vertebrates is temporally congruent with dipterocarp forest development. Biol Lett 8:994–7.

Herre AW. 1958. On the gliding of flying lizards genus *Draco*. Copeia 1958:338.

Higham TE, Russell AP, Niklas KJ. 2017. Leaping lizards landing on leaves: escape-induced jumps in the rainforest canopy challenge the adhesive limits of geckos. J R Soc Interface 14:20170156.

Hoerner SF. 1965. Fluid-dynamic drag. Brick Town (NJ): Hoerner Fluid Dynamics.

Hunt KD, Cant JG, Gebo DL, Rose MD, Walker SE, Youlatos D. 1996. Standardized descriptions of primate locomotor and postural modes. Primates 37:363–87.

Irschick DJ, Losos JB. 1998. A comparative analysis of the ecological significance of maximal locomotor performance in Caribbean Anolis lizards. Evolution 52:219–26.

Jusufi A, Kawano DT, Libby T, Full RJ. 2010. Righting and turning in mid-air using appendage inertia: reptile tails, analytical models and bio-inspired robots. Bioinspir Biomim 5:045001.

Jusufi A, Goldman DI, Revzen S, Full RJ. 2008. Active tails enhance arboreal acrobatics in geckos. Proc Natl Acad Sci USA 105:4215–9.

Khandelwal PC, Hedrick TL. 2020. How biomechanics, path planning and sensing enable gliding flight in a natural environment. Proc R Soc B Biol Sci 287:20192888.

Libby T, Moore TY, Chang-Siu E, Li D, Cohen DJ, Jusufi A, Full RJ. 2012. Tail-assisted pitch control in lizards, robots and dinosaurs. Nature 481:181–4.

Mcguire JA, Dudley R. 2011. The biology of gliding in flying lizards (genus *Draco*) and their fossil and extant analogs. Integr Comp Biol 51:983–90.

Mcguire JA, Heang KB. 2001. Phylogenetic systematics of Southeast Asian flying lizards (Iguania: Agamidae: *Draco*) as inferred from mitochondrial DNA sequence data. Biol J Linn Soc 72:203–29.

Mcguire J. 2003. Allometric prediction of locomotor performance: an example from southeast Asian flying lizards. Am Nat 161:337–49.

Mcguire J, Dudley R. 2005. The cost of living large: comparative gliding performance in flying lizards (Agamidae: *Draco*). Am Nat 166:93–106.

Russell AP. 1979. The origin of parachuting locomotion in gekkonid lizards (Reptilia: Gekkonidae). Zool J Linn Soc 65:233–49.

Russell AP, Dijkstra LD, Powell GL. 2001. Structural characteristics of the patagium of *Ptychozoon kuhli* (Reptilia: Gekkonidae) in relation to parachuting locomotion. J Morphol 247:252–63.

Russell AP, Dijkstra LD. 2001. Patagial morphology of *Draco volans* (Reptilia: Agamidae) and the origin of glissant locomotion in flying dragons. J Zool 253:457–71.

Shin WD, Park J, Park H. 2018. Bio-inspired design of a gliding-walking multi-modal robot. IEEE/RSJ International Conference on Intelligent Robots and Systems (IROS).IEEE, Madrid, Spain.

Smith JM. 1952. The importance of the nervous system in the evolution of animal flight. Evolution 6:127–9.

Socha JJ. 2005. A 3-D kinematic analysis of gliding in a flying snake, *Chrysopelea paradisi*. J Exp Biol 208:1817–33.

Socha JJ. 2002. Gliding flight in the paradise tree snake. Nature 418:603–4.

Socha JJ, Jafari F, Munk Y, Byrnes G. 2015. How animals glide: from trajectory to morphology. Can J Zool 93:901–24.

Vogel S. 1994. Life in moving fluids. Princeton (NJ): Princeton University Press.

Yanoviak SP, Dudley R, Kaspari M. 2005. Directed aerial descent in canopy ants. Nature 433:624–6.

Yeaton IJ, Ross SD, Baumgardner GA, Socha JJ. 2020. Undulation enables gliding in flying snakes. Nat Phys 16:974–82.

Yeaton IJ, Socha JJ, Ross SD. 2017. Global dynamics of non-equilibrium gliding in animals. Bioinspir Biomim 12:026013.

Young BA, Lee CE, Daley KM. 2002. On a Flap and a Foot: Aerial Locomotion in the "Flying" Gecko, Ptychozoon kuhli. J Herpetol 36:412–8.

Zhao F, Wang W, Zhang J, Wyrwa J, Sun F. 2019. Aerodynamic characteristics and pitching adjusting mechanism of the flying squirrel with deployed patagium. IEEE Access 7:185554–64.